Supporting Information to

Boron Difluorides with Formazanate Ligands: Redox-Switchable Fluorescent Dyes with Large Stokes Shifts

M.-C. Chang,[a] A. Chantzis,[b] D. Jacquemin[b,c] and E. Otten[a*]

[a.] Stratingh Institute for Chemistry, University of Groningen, Nijenborgh 4, 9747 AG Groningen, The Netherlands
E-mail: edwin.otten@rug.nl
[b.] Laboratoire CEISAM - UMR CNRS 6230, Université de Nantes, 2 Rue de la Houssinière, BP 92208, 44322 Nantes Cedex 3, France
[c.] Institut Universitaire de France, 1, rue Descartes, 75005 Paris Cedex 5, France

Contents

Experimental Section 3
X-ray crystallography 6
Computational details 10
References 12

Experimental Section

General Considerations. All manipulations were carried out under nitrogen atmosphere using standard glovebox, Schlenk, and vacuum-line techniques. Toluene, hexane, and pentane (Aldrich, anhydrous, 99.8%) were passed over columns of Al_2O_3 (Fluka), BASF R3-11-supported Cu oxygen scavenger, and molecular sieves (Aldrich, 4 Å). Diethyl ether and THF (Aldrich, anhydrous, 99.8%) were dried by percolation over columns of Al_2O_3 (Fluka). Deuterated solvents were vacuum transferred from Na/K alloy (C_6D_6, THF-d_8, Aldrich) and stored under nitrogen. The compounds $(C_6F_5NNC(p\text{-tolyl})NNMes)_2Zn$,[1] (PhNNC(*p*-tolyl)NNPh)BF_2 (**1a**),[2] (PhNNC(C_6F_5)NNMes)BF_2 (**1f**),[2] (PhNNC(CN)NNPh)BF_2 (**1h**),[3] $[Cp_2Co][(PhNNC(p\text{-tolyl})NNPh)BF_2]$ ($[Cp_2Co]$**[1a]**$^{\bullet-}$),[2] and the formazan ligands were synthesized according to published procedures.[1,4] The phenylene-linked compounds **1j** and **1k** were published by Gilroy and co-workers while this work was in progress;[5] our synthetic procedures are very similar and give comparable results, and are not therefor not reproduced here. $BF_3(Et_2O)$ was purchased from Aldrich and used as received. NMR spectra were recorded on Mercury 400, Inova 500 or Agilent 400 MR spectrometers. The ^1H and ^{13}C NMR spectra were referenced internally using the residual solvent resonances and reported in ppm relative to TMS (0 ppm); *J* is reported in Hz. Assignment of NMR resonances was aided by gradient-selected COSY, NOESY, HSQCAD and/or HMBCAD experiments using standard pulse sequences. ^{11}B NMR spectra were recorded in quartz (or normal glass) NMR tubes using a OneNMR probe on an Agilent 400 MR system. UV-Vis spectra were recorded in THF solution (~ 10-5 M) using a Avantes AvaSpec 3648 spectrometer and AvaLight-DHS lightsource inside a N_2 atmosphere glovebox. The photoluminescence quantum yields were determined using optically dilute solutions in THF (λ_{ex} = 473 nm) with optically dilute $Ru(bipy)_3$ aqueous solution as reference. Spectra were recorded using a 75W Xenon lamp coupled to a Zolix 150 monochromator coupled directly to a Qpod cuvette holder (Quantum Northwest) and emission was collected through a fibre optic connected Shamrock 163 spectrograph and iDUS-420A-OE CCD detector. Spectra are uncorrected for instrument response. Elemental analyses were performed at the Microanalytical Departement of the University of Groningen or Kolbe Microanalytical Laboratory (Mülheim an der Ruhr, Germany).

General Procedure for (formazanate)BF_2 complexes

Indirect Method (A).

A schlenk tube was charged with formazan, 0.5 equivalents of dimethylzinc (1.2M in toluene) and dry toluene. The reaction mixture was stirred overnight at RT, and then all volatiles were removed under vacuum. At this stage, the corresponding bis(formazanate) zinc complex is formed. Without further workup, to the crude reaction mixture $BF_3(OEt_2)$ was added (1.5-2.0 eq vs. formazan) as a solution in toluene. After the reaction mixture had been stirred overnight at 70 °C, all volatiles were removed under vacuum. The product was purified by chromatography (DCM/hexane, silica gel) or recrystallization from hexane or heptane.
Similarly, the products may be obtained from reaction of isolated bis(formazanate)zinc complex with $BF_3(OEt_2)$.

Direct Method (B).[3,6]

A schlenk flask was charged with formazan and dry toluene. Triethylamine (3 eq vs. formazan) was then added slowly at RT, and the reaction mixture was stirred for 10-20 min. Then, boron trifluoride diethyl etherate (5 eq vs. formazan) was added, and the solution was stirred at 80 °C for 24 hours. After the solution had been cooled to room temperature, deionized water was added to quench the reaction. The toluene solution was washed with deionized water three times, dried over $MgSO_4$, gravity filtered and the volatiles were evaporated. The crude product was purified by flash chromatography (DCM, silica gel). The product can be further purified by recrystallization from hexane or heptane.

(PhNNC(^{t}Bu)NNPh)BF_2 (1b). [PhNNC(^{t}Bu)NNHPh] (336.5 mg, 1.2 mmol), dimethylzinc (1.2M solution in toluene, 0.5 mL, 0.6 mmol) and boron trifluoride diethyl etherate (0.25 mL, 2.0 mmol) were used (method A). After recrystallization from hexane, compound **1b** was obtained as orange crystals (260.9 mg, 66.2 %). ^1H NMR (400 MHz, $CDCl_3$, 25 °C): 7.79 (d, 4H, *J* = 6.0 Hz, Ph *o*-H), 7.42 (t, 4H, *J* = 6.4 Hz, Ph *m*-H), 7.36 (t, 2H, *J* = 6.0 Hz, Ph *p*-H), 1.45 (s, 9H, tBu). ^{13}C NMR (100.6 MHz, $CDCl_3$, 25 °C): 158.9 (N*C*N), 144.1 (Ph *i*-C), 129.4 (Ph *p*-CH), 129.2 (Ph *m*-CH), 123.4 (Ph *o*-CH), 37.0 (tBu *C*$(CH_3)_3$), 29.8 (tBu *C*H_3). ^{19}F NMR (376.4 MHz, $CDCl_3$, 25 °C): -145.7 (q, 2F, *J* = 28.9 Hz, BF_2). ^{11}B NMR (128.3 MHz, $CDCl_3$, 25 °C): -0.70 (t, 1B, *J* = 28.7 Hz, BF_2). Anal. calcd for $C_{17}H_{19}BF_2N_4$: C, 62.22; H, 5.84; N, 17.07. Found: C, 62.37; H, 5.82; N, 16.90.

[PhNNC(p-tolyl)NNMes]BF_2 (1c). [PhNNC(p-tolyl)NNHMes] (255.2 mg, 0.72 mmol), dimethylzinc (1.2M solution in toluene, 0.3 mL, 0.36 mmol) and boron trifluoride diethyl etherate (0.15 mL, 1.22 mmol) were used (method A). After chromatography (DCM/hexane: 2/5, silicagel, R_f: 0.4), compound **1c** was obtained as deep red solid (182.0 mg, 63 %). ^1H NMR (400 MHz, $CDCl_3$, 25 °C): 7.94 (d, 2H, *J* = 8.4 Hz, p-tolyl CH), 7.83 (d, 2H, *J* = 7.2 Hz, Ph *o*-CH), 7.49-7.38 (m, 3H, Ph *m*- and *p*-CH), 7.24 (d, 2H, *J* = 8.0 Hz, p-tolyl CH), 6.92 (s, 2H, Mes *m*-CH), 2.41 (s, 3H, p-tolyl CH_3), 2.30 (s, 3H, Mes *p*-CH_3), 2.05 (s, 6H, Mes *o*-CH_3). ^{13}C NMR (100.6 MHz, $CDCl_3$, 25 °C): 151.4 (NCN), 143.3 (Ph *i*-C), 139.8 (p-tolyl *p*-C), 139.8 (Mes *o*-C), 139.3 (Mes *p*-C), 134.7 (Mes *i*-C), 130.4 (p-tolyl *i*-C), 129.7 (Ph *p*-CH), 129.6 (p-tolyl CH), 129.5 (Mes *m*-CH), 129.3 (Ph *m*-CH), 125.8 (p-tolyl CH), 123.9 (Ph *o*-CH), 21.6 (p-tolyl *p*-CH_3), 21.3 (Mes *p*-CH_3), 18.0 (Mes *o*-CH_3). ^{19}F NMR (376.4 MHz, $CDCl_3$, 25 °C): -156.9 (q, 2F, *J* = 23.5 Hz, BF_2). ^{11}B NMR (128.3 MHz, $CDCl_3$, 25 °C): -1.07 (t, 1B, *J* = 23.6 Hz, BF_2). Anal. calcd for $C_{23}H_{23}BF_2N_4$: C, 68.33; H, 5.73; N, 13.86. Found: C, 68.65; H, 5.83; N, 13.57.

[PhNNC(*p*-tolyl)NNC_6F_5]BF_2 (1d). [PhNNC(p-tolyl)NNHC_6F_5] (536 mg, 1.33 mmol), dimethylzinc (1.2M solution in toluene, 0.5 mL, 0.6 mmol) and boron trifluoride diethyl etherate (0.3 mL, 2.45 mmol) were used (method A). After recrystallization from hexane, compound **1d** was obtained as orange crystals (525.7 mg, 87.7 %). ^1H NMR (400 MHz, $CDCl_3$, 25 °C): 8.01 (d, 2H, *J* = 8.4 Hz, p-tolyl CH), 7.76-7.74 (m, 2H, Ph *o*-H), 7.04 8.01 (d, 2H, *J* = 8.0 Hz, p-tolyl CH), 6.94-6.90 (m, 3H, Ph *m*-H and *p*-H), 2.09 (s, 3H, p-tolyl CH_3). ^{13}C NMR (100.6 MHz, $CDCl_3$, 25 °C): 153.1 (N*C*N), 144.2 (dm, *J* = 255.5 Hz, C_6F_5), 143.9 (m, Ph *i*-C), 141.9 (dm, *J* = 257.5 Hz, C_6F_5), 140.9 (p-tolyl *i*-C), 138.2 (dm, *J* = 250.9 Hz, C_6F_5), 131.7 (Ph *m*-CH), 130.4 (*p*-tolyl *C*Me), 130.3 (*p*-tolyl CH), 129.8 (Ph *p*-CH), 126.6 (*p*-tolyl CH), 124.9 (t, *J* = 2.0 Hz, Ph *o*-CH), 119.4 (m,

C_6F_5 *i*-C), 21.6 (*p*-tolyl CH_3). ^{19}F NMR (376.4 MHz, $CDCl_3$, 25 °C): -147.8 – 147.9 (m, 2F, C_6F_5 *m*-CF), -153.0 (t, 1F, *J* = 22.5 Hz, C_6F_5 *p*-CF), -154.4 (q, 2F, *J* = 24.0 Hz, BF_2), -161.5 - -161.6 (m, 2F, C_6F_5 *o*-CF). ^{11}B NMR (128.3 MHz, $CDCl_3$, 25 °C): -1.06 (t, 1B, *J* = 23.7 Hz, BF_2). Anal. calcd for $C_{20}H_{12}BF_7N_4$: C, 53.13; H, 2.68; N, 12.39. Found: C, 53.50; H, 2.72; N, 12.14.

[C_6F_5NNC(*p*-tolyl)NNMes]BF_2 (1e). [C_6F_5NNC(*p*-tolyl)NNMes]$_2$Zn (535 mg, 0.56 mmol) and boron trifluoride diethyl etherate (0.24 mL, 1.9 mmol) were used (method A). The product was purified by flash chromatography (DCM, silicagel), to afford **1e** as an orange solid (439.6 mg, 79.7 %). ^1H NMR (400 MHz, $CDCl_3$, 25 °C): 7.83 (d, 2H, *J* = 8.0 Hz, p-tolyl CH), 7.25 (d, 2H, *J* = 7.7 Hz, p-tolyl CH, overlap with $CDCl_3$), 6.96 (s, 2H, Mes *m*-CH), 2.40 (s, 3H, *p*-tolyl CH_3), 2.32 (s, 3H, Mes *p*-CH_3), 2.13 (s, 6H, Mes *o*-CH_3). ^{13}C NMR (100.6 MHz, $CDCl_3$, 25 °C): 152.6-152.2 (m, N*C*N), 143.8 (dm, *J* = 255.8 Hz, C_6F_5), 141.9 (dm, *J* = 246.2 Hz, C_6F_5), 140.7 (Mes *p*-C), 140.4 (p-tolyl *i*-C), 139.9 (Mes *i*-C), 138.2 (dm, *J* = 251.2 Hz, C_6F_5), 134.4 (Mes *o*-C), 129.9 (Mes *m*-CH), 129.8 (p-tolyl CH), 129.4 (p-tolyl *i*-C), 126.0 (p-tolyl CH), 119.0-118.5 (m, C_6F_5 *i*-C), 21.6 (p-tolyl CH_3), 21.3 (Mes *p*-CH_3), 18.0 (Mes *o*-CH_3). ^{19}F NMR (376.4 MHz, $CDCl_3$, 25 °C): -146.4 – 146.6 (m, 2F, C_6F_5 *m*-CF), -152.2 (t, 1F, *J* = 21.3 Hz, C_6F_5 *p*-CF), -159.4 (qt, 2F, *J* = 21.3, 6.1 Hz, BF_2), -160.9 - -161.1 (m, 2F, C_6F_5 *o*-CF). ^{11}B NMR (128.3 MHz, $CDCl_3$, 25 °C): -2.06 (t, 1B, *J* = 20.9 Hz, BF_2). Anal. calcd for $C_{23}H_{18}BF_7N_4$: C, 55.90; H, 3.67; N, 11.34. Found: C, 56.01; H, 3.64; N, 11.03.

[C_6F_5NNC(C_6F_5)NNMes]BF_2 (1g). [C_6F_5NNC(C_6F_5)NNHMes] (301.3 mg, 0.58 mmol), triethylamine (0.24 mL, 1.72 mmol) and boron trifluoride diethyl etherate (0.35 mL, 2.84 mmol) were used (method B). After chromatography (DCM/hexane: 1/5, silicagel, R_f: 0.5), compound **1g** was obtained as orange crystals (290.5 mg, 88.3 %). ^1H NMR (400 MHz, $CDCl_3$, 25 °C): 6.95 (s, 4H, Mes *m*-CH), 2.30 (s, 6H, Mes *p*-CH_3), 2.13 (s, 12H, Mes *o*-CH_3). ^{13}C NMR (100.6 MHz, $CDCl_3$, 25 °C): 146.9 (m, NCN), 143.7 (dm, *J* = 256.5 Hz, C_6F_5), 143.2 (dm, *J* = 250.1 Hz, C_6F_5), 143.6 (dm, *J* = 255.4 Hz, C_6F_5), 142.4 (dm, *J* = 258.8 Hz, C_6F_5), 141.0(Mes *p*-C), 139.5 (Mes *i*-C), 138.1 (dm, *J* = 251.5 H, C_6F_5), 134.3 (Mes *o*-C), 130.0 (Mes *m*-CH), 118.1 (m, C_6F_5 *i*-C), 108.7 (m, C_6F_5 *i*-C), 21.3 (Mes *p*-CH_3), 17.8 (Mes *o*-CH_3). ^{19}F NMR (376.4 MHz, $CDCl_3$, 25 °C): -140.6 (dd, 2F, *J* = 22.8, 7.4 Hz, C_6F_5 *o*-CF), -146.4 (m, 2F, C_6F_5 *o*-CF), -150.3 - -150.5 (m, 2F, C_6F_5 *p*-CF and C_6F_5 *p*-CF), -158.1 (qt, 2F, *J* = 20.9, 6.1 Hz, BF_2), -160.2 - -160.4 (m, 2F, C_6F_5 *m*-CF), -160.7 - -160.9 (m, 2F, C_6F_5 *m*-CF). ^{11}B NMR (128.3 MHz, $CDCl_3$, 25 °C): -2.28 (t, 1B, *J* = 20.3 Hz, BF_2). Anal. calcd for $C_{22}H_{11}BF_{12}N_4$: C, 46.35; H, 1.94; N, 9.83. Found: C, 46.77; H, 2.00; N, 9.55.

[PhNNC(CN(B(C_6F_5)$_3$))NNPh]BF_2 1h^{BCF}. A vial was charged with [PhNNC(CN)NNPh]BF_2 (**1h**) (99.5 mg, 0.33 mmol), B(C_6F_5)$_3$ (178.2 mg, 0.35 mmol) and toluene and then the reaction mixture was stirred at room temperature for 1 hour. The crude product was recrystallized by slow diffusion of hexane into the reaction mixture at -30 °C to afford compound **1h^{BCF}** as orange crystals (237.1 mg, 88.8 %). ^1H NMR (400 MHz, $CDCl_3$, 25 °C): 7.70-7.64 (m, 4H, Ph *o*-CH), 6.85-6.79 (m, 6H, Ph *m*-CH and *p*-CH). ^{13}C NMR (100.6 MHz, $CDCl_3$, 25 °C): 148.2 (dm, *J* = 238.4 Hz, C_6F_5), 142.6 (Ph *i*-C), 140.7 (dm, *J* = 253.6 Hz, C_6F_5), 137.5 (dm, *J* = 249.6 Hz, C_6F_5), 132.2 (Ph *p*-CH)., 129.4 (Ph *m*-CH)., 122.6 (Ph *o*-CH). ^{19}F NMR (376.4 MHz, $CDCl_3$, 25 °C): -125.8 (q, 2F, *J* = 29.4 Hz, BF_2), -134.1 (dd, 6F, *J* = 23.5, 9.9 Hz, C_6F_5 *o*-CF), -154.8 (t, 3F, *J* = 21.0 Hz, C_6F_5 *p*-CF), -162.8 (td, 6F, *J* = 22.2, 8.6 Hz, C_6F_5 *m*-CF). ^{11}B NMR (128.3 MHz, $CDCl_3$, 25 °C): -0.76 (t, 1B, *J* = 31.6 Hz, BF_2).

[MesNNC(CN)NNMes]BF_2 (1i). [MesNNC(CN)NNHMes] (200.6 mg, 0.60 mmol), triethylamine (0.25 mL, 1.80 mmol) and boron trifluoride diethyl etherate (0.39 mL, 3.16 mmol) were used (method B). After flash chromatography (DCM, silicagel) and recrystallization from heptane, compound **1i** was obtained as yellow crystals (188.8 mg, 82.3 %). ^1H NMR (400 MHz, $CDCl_3$, 25 °C): 6.94 (s, 4H, Mes *m*-CH), 2.30 (s, 6H, Mes *p*-CH_3), 2.17 (s, 12H, Mes *o*-CH_3). ^{13}C NMR (100.6 MHz, $CDCl_3$, 25 °C): 140.4 (Mes *p*-C), 139.0 (Mes *i*-C), 134.1 (Mes *o*-C), 130.2 (Mes *m*-CH), 129.1 (N*C*N), 113.8 (CN), 21.2 (Mes *p*-CH_3), 18.5 (Mes *o*-CH_3). ^{19}F NMR (376.4 MHz, $CDCl_3$, 25 °C): -145.6 (q, 2F, *J* = 23.8 Hz, BF_2). ^{11}B NMR (128.3 MHz, $CDCl_3$, 25 °C): -2.28 (t, 1B, *J* = 23.7 Hz, BF_2). Anal. calcd for $C_{20}H_{22}BF_2N_5$: C, 63.01; H, 5.82; N, 18.37. Found: C, 63.02; H, 5.79; N, 18.17.

[Cp_2Co]$^+$[1b]$^{\bullet-}$. A vial was charged with 30.0 mg of **1b** (0.09 mmol) and 2 mL of THF. A solution of 17.5 mg of Cp_2Co (0.09 mmol) in 2 mL of THF was slowly added to the vial. After the reaction mixture was allowed to stand at RT for 6 hours, 10 mL of hexane was slowly added. After diffusion of the hexane layer into the reaction mixture, compound **[Cp_2Co]$^+$[1b]$^{\bullet-}$** was obtained as deep green crystals (47.0 mg, 0.09 mmol, 99 %).

[Na(15-crown-5)]$^+$[1c]$^{\bullet-}$. A vial was charged with 12.1 mg of **1c** (0.03 mmol), 28.4 mg of Na/Hg (2.447 % of Na, 0.03 mmol), 6.1 µL of 15-crown-5 (0.03 mmol) and 1.5 mL of THF. After the reaction mixture had been stirred at RT for 6 hours, the supernatant was separated from Hg(l). Addition of a layer of hexane on top of the reaction mixture, followed by slow diffusion of the layers gave compound **[Na(15-crown-5)]$^+$[1c]$^{\bullet-}$** as green crystals (17 mg, 0.026 mmol, 88%).

[Cp_2Co]$^+$[1f]$^{\bullet-}$. Following a similar procedure as above (using 29.8 mg of **1f** (0.06 mmol) and 13.4 mg of Cp_2Co (0.07 mmol)), compound **[Cp_2Co]$^+$[1f]$^{\bullet-}$** was obtained (41.1 mg, 0.06 mmol, 99 %).

[Cp_2Co]$^+_2$[1j]$^{2-}$. Following a similar procedure as above (using 19.7 mg of **1j** (0.03 mmol) and 14.4 mg of Cp_2Co (0.08 mmol)), compound **[Cp_2Co]$^+_2$[1j]$^{2-}$** was obtained (30.1 mg, 0.03 mmol, 99 %). Crystals suitable for X-ray analysis may be obtained in a similar manner using Cp^*_2Co instead of Cp_2Co, and using a THF/toluene solvent mixture.

[Cp_2Co]$^+_2$[1k]$^{2-}$. Following a similar procedure as above (using 19.8 mg of **1k** (0.03 mmol) and 14.6 mg of Cp_2Co (0.08 mmol)), compound **[Cp_2Co]$^+_2$[1k]$^{2-}$** was obtained (32.4 mg, 0.03 mmol, 99 %).

NMR spectral data

[PhNNC(^{t}Bu)NNPh]BF_2 (1b)

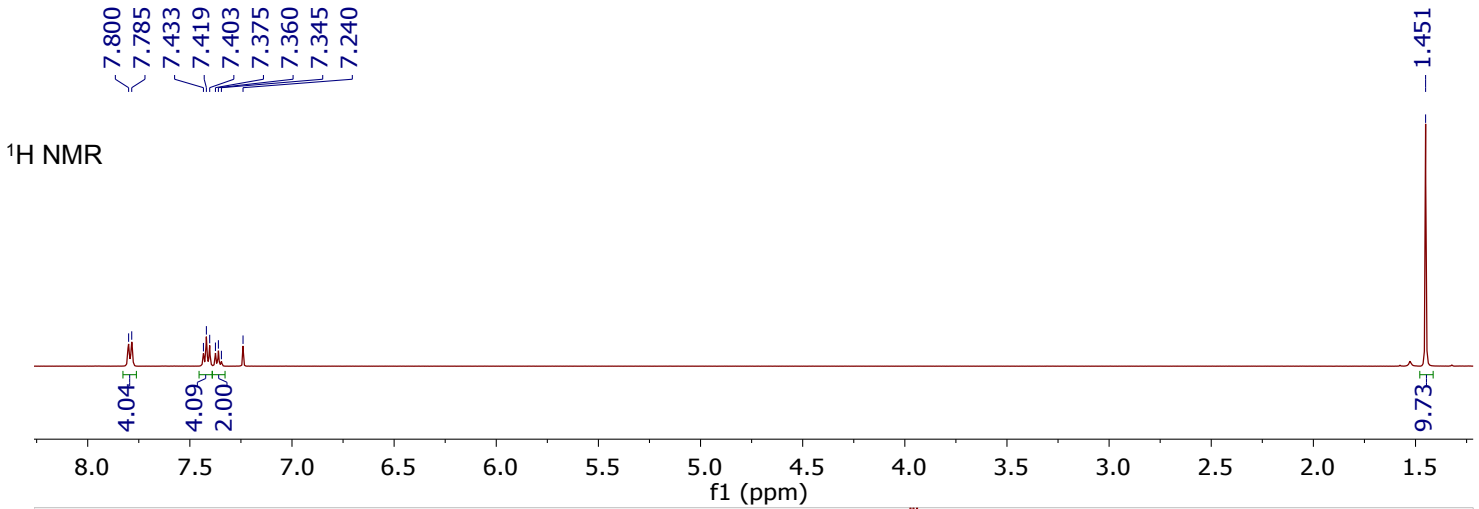

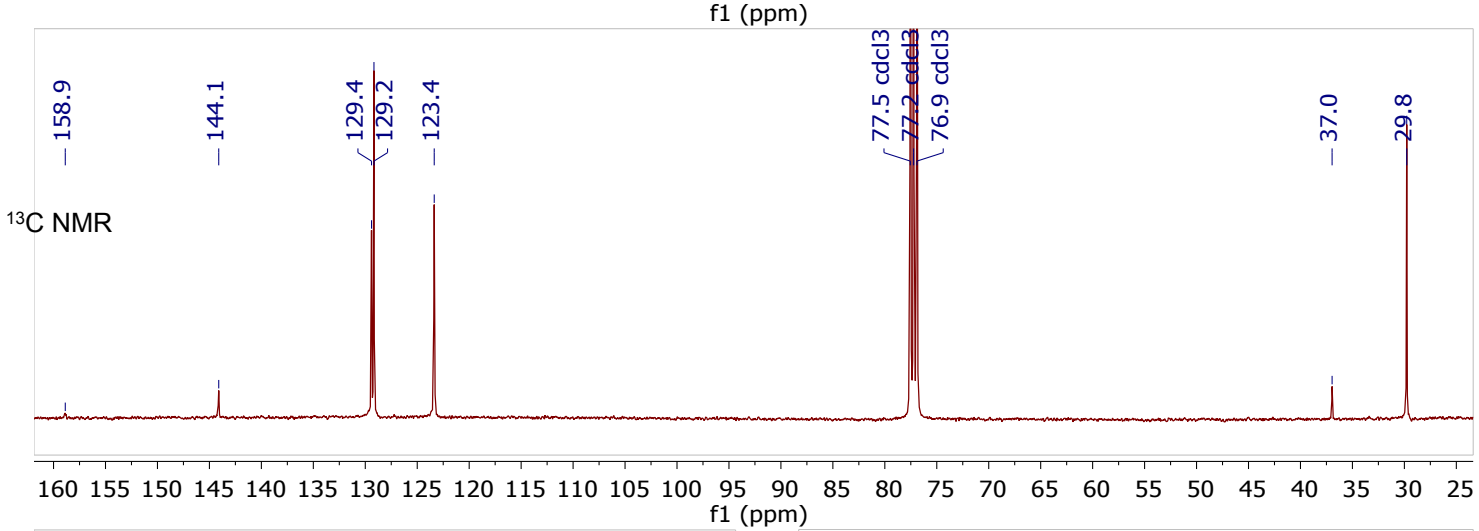

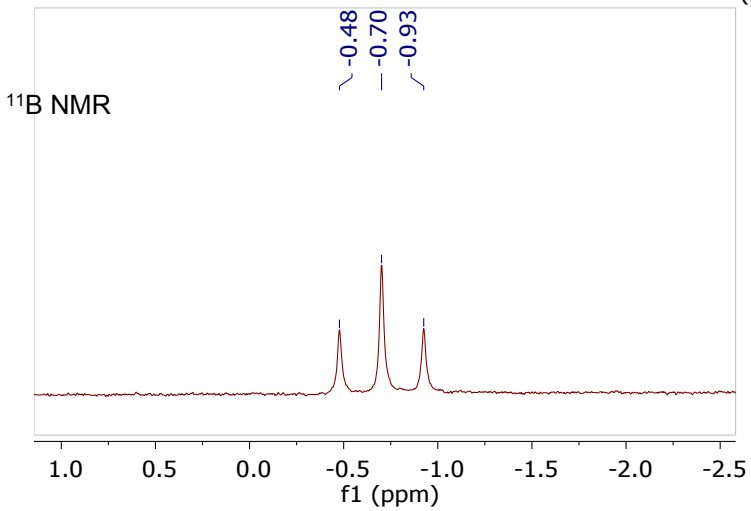

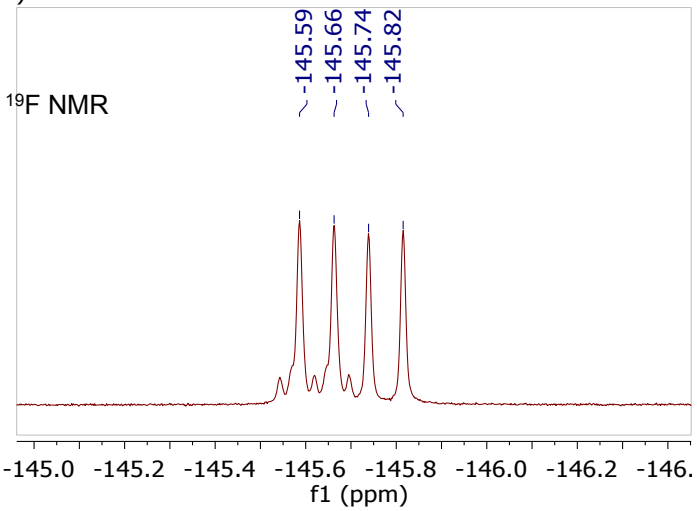

[PhNNC(p-tolyl)NNMes]BF_2 (1c)

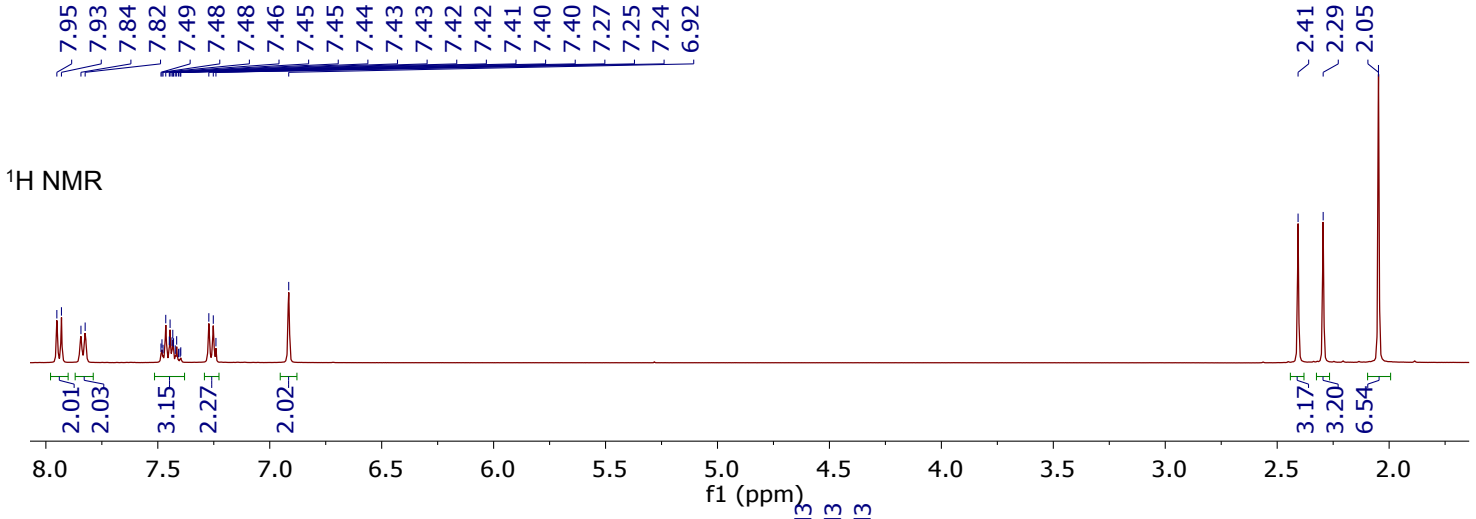

^{1}H NMR

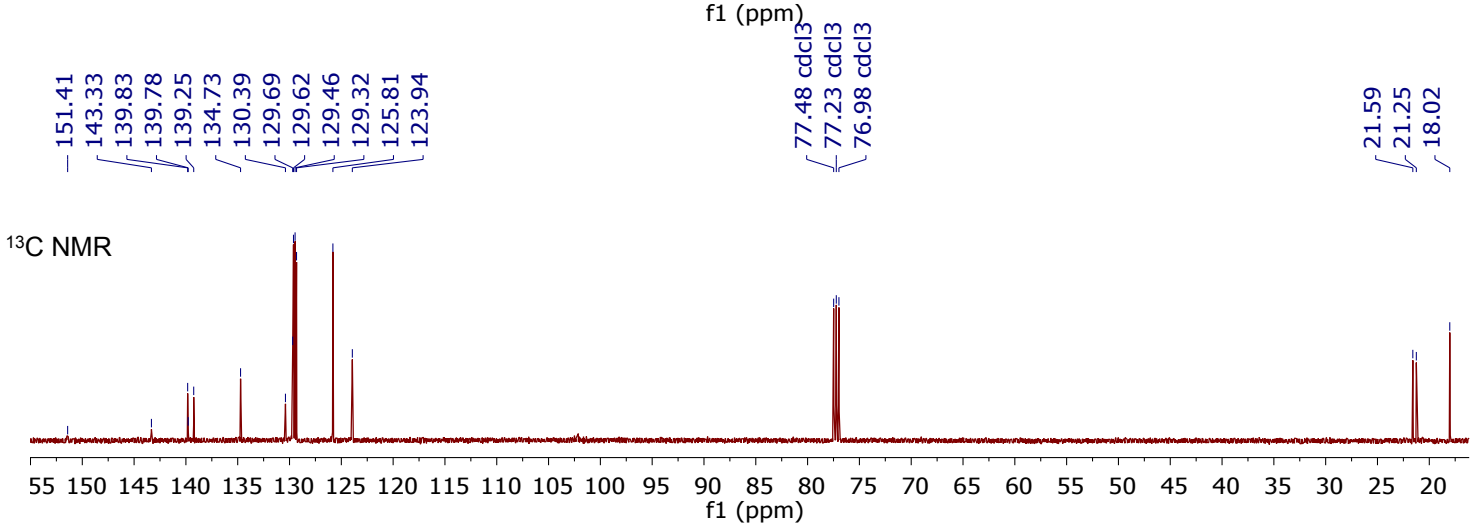

^{13}C NMR

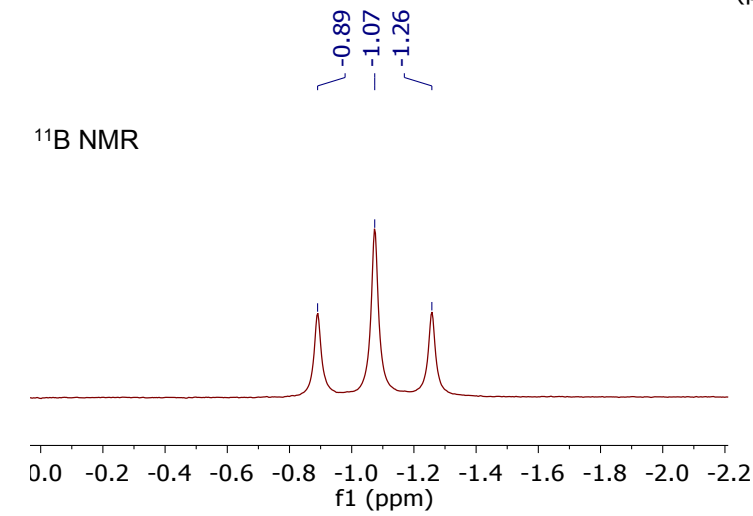

^{11}B NMR

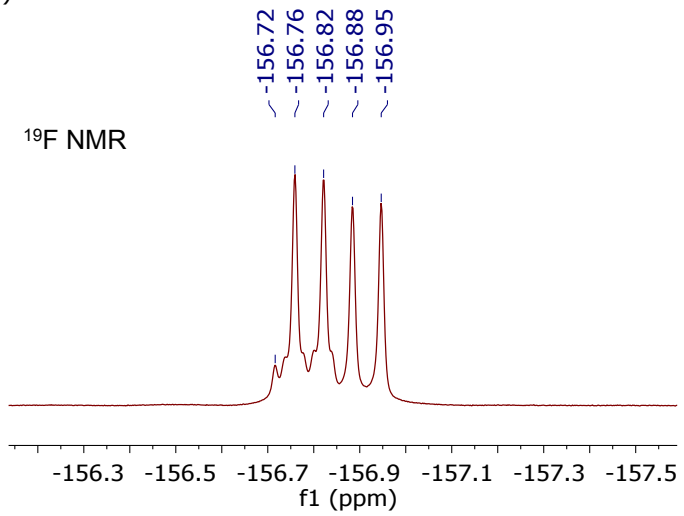

^{19}F NMR

[PhNNC(p-tolyl)NNC$_6$F$_5$]BF$_2$ (1d)

^{1}H NMR

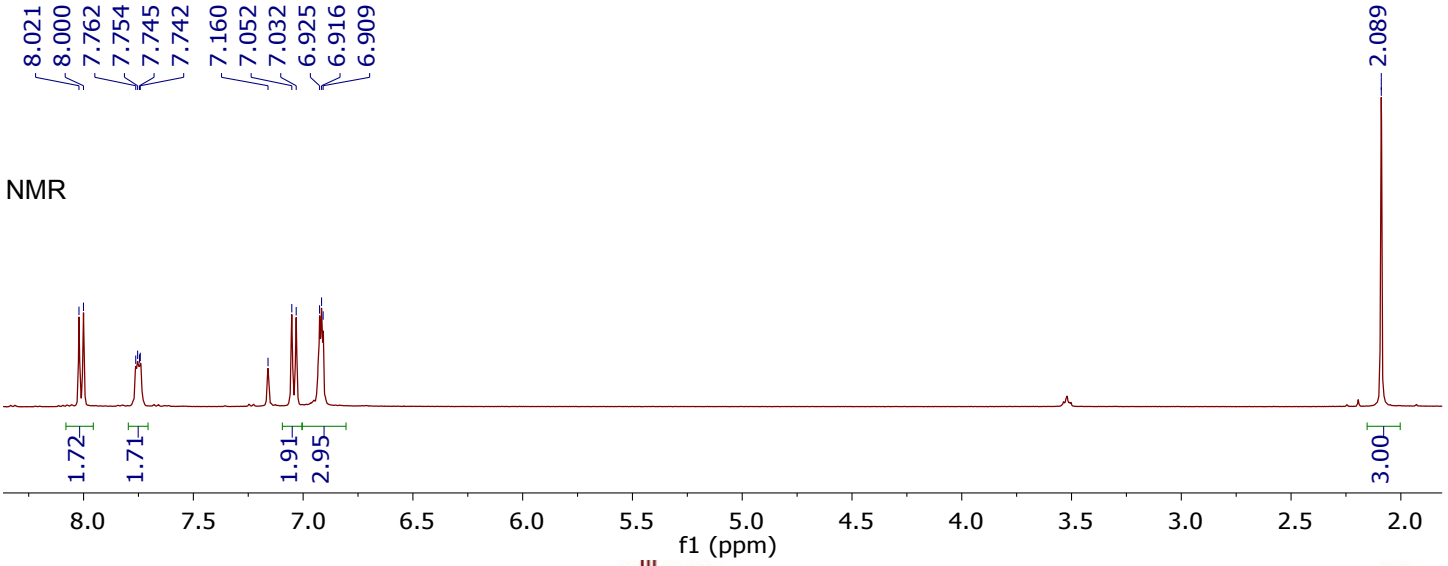

^{13}C NMR

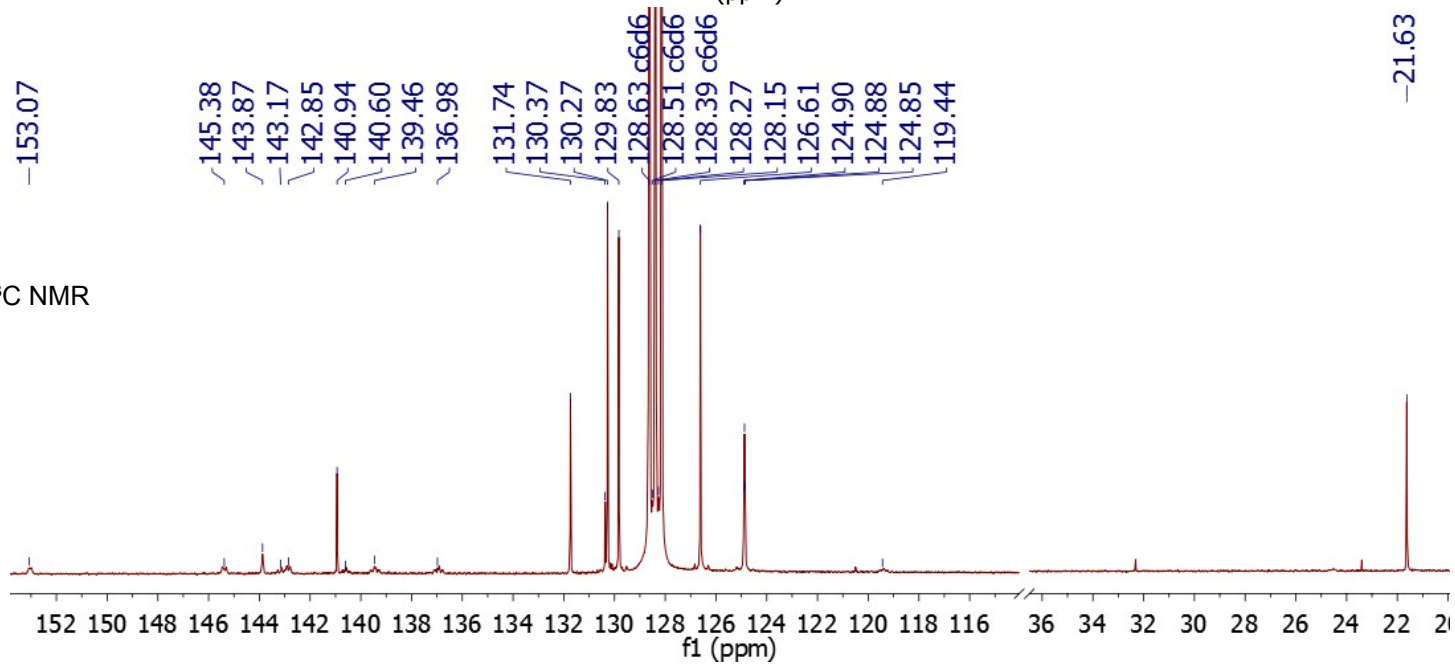

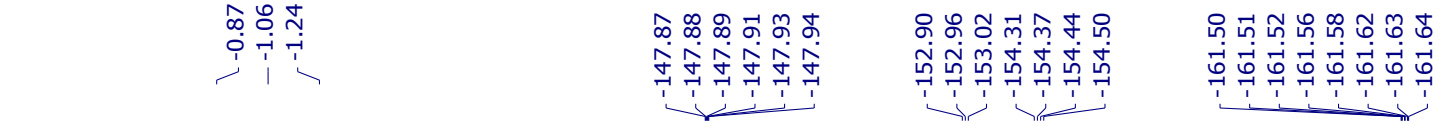

^{11}B NMR

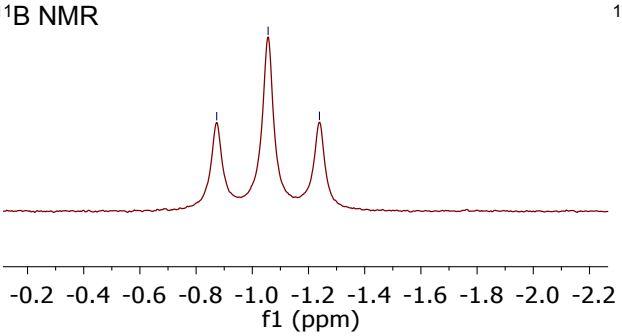

^{19}F NMR

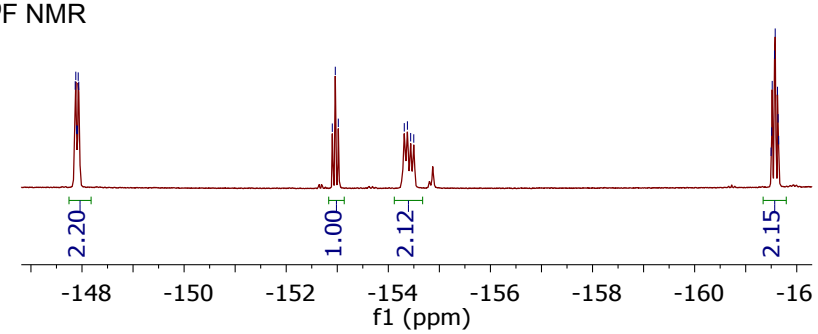

[C_6F_5NNC(p-tolyl)NNMes]BF_2 (1e)

^{1}H NMR

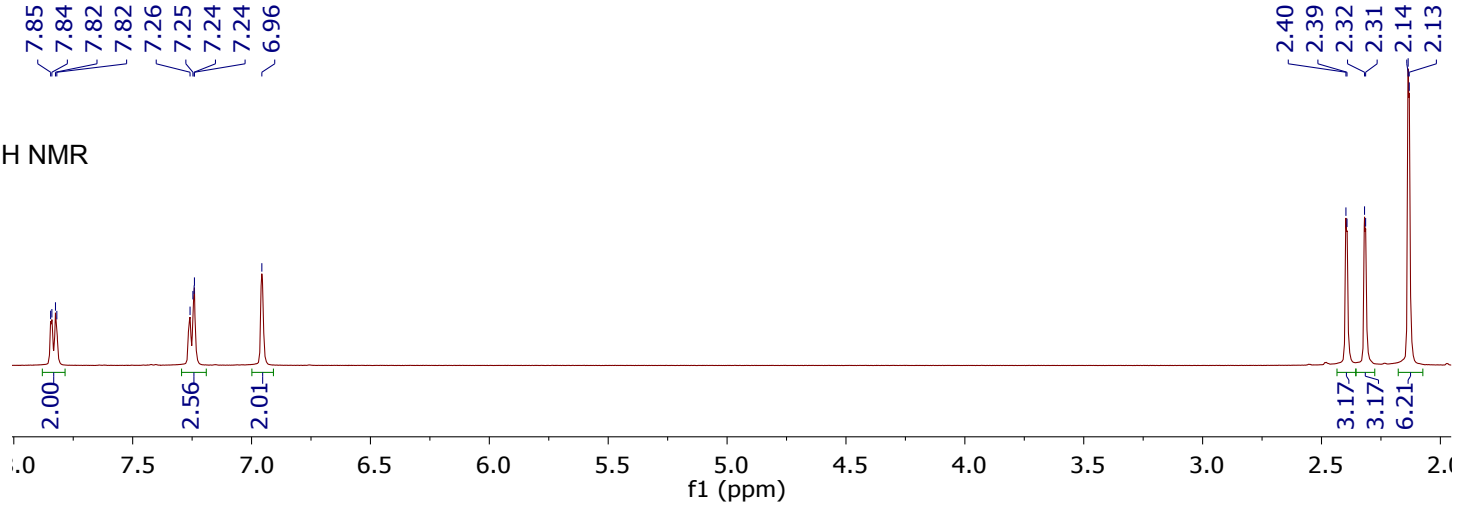

^{13}C NMR

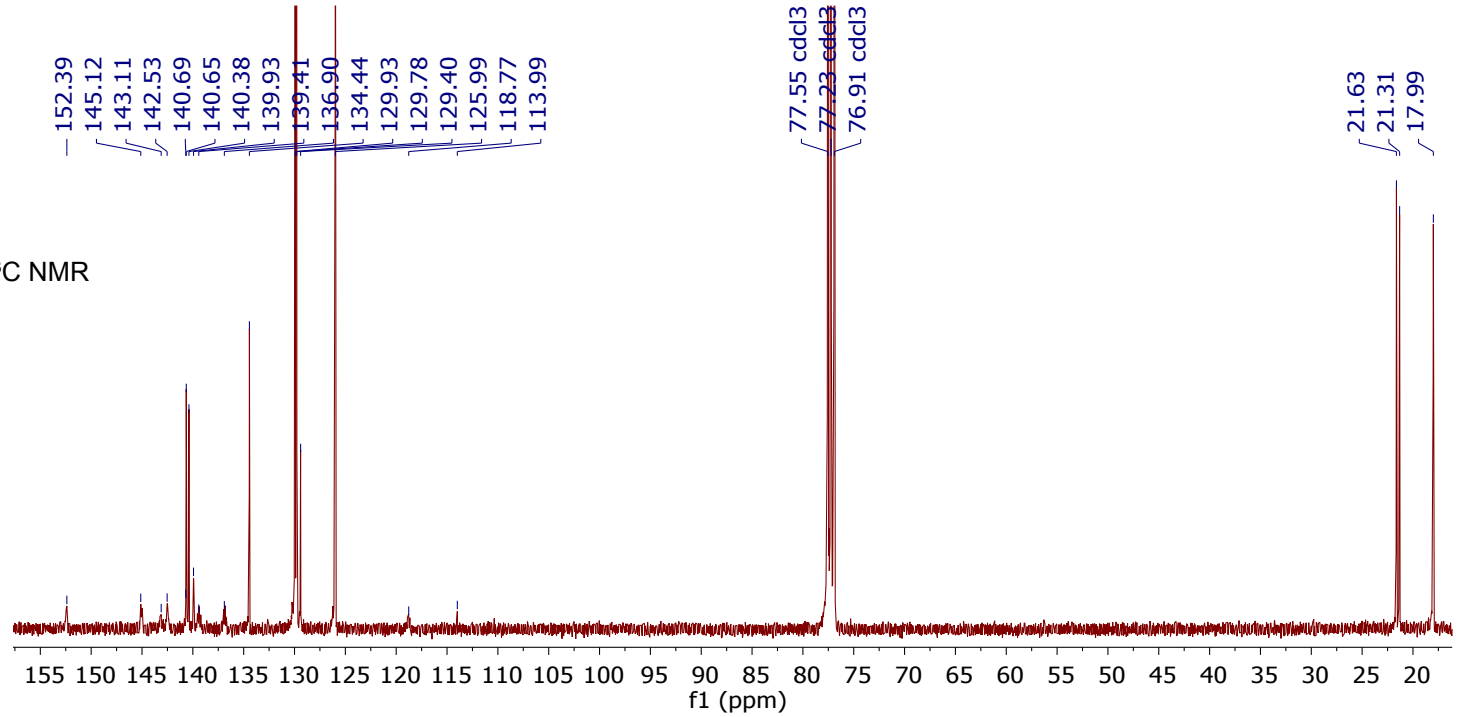

^{11}B NMR

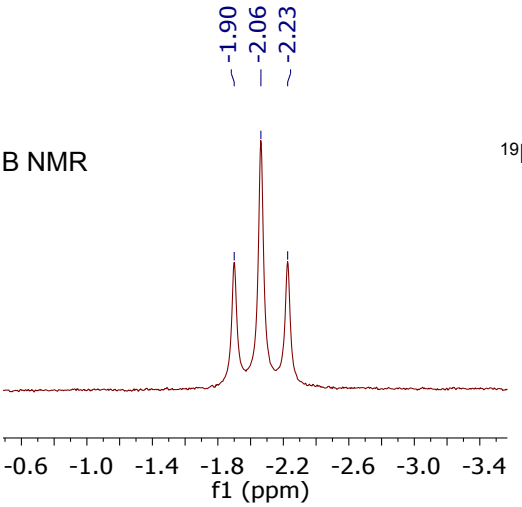

^{19}F NMR

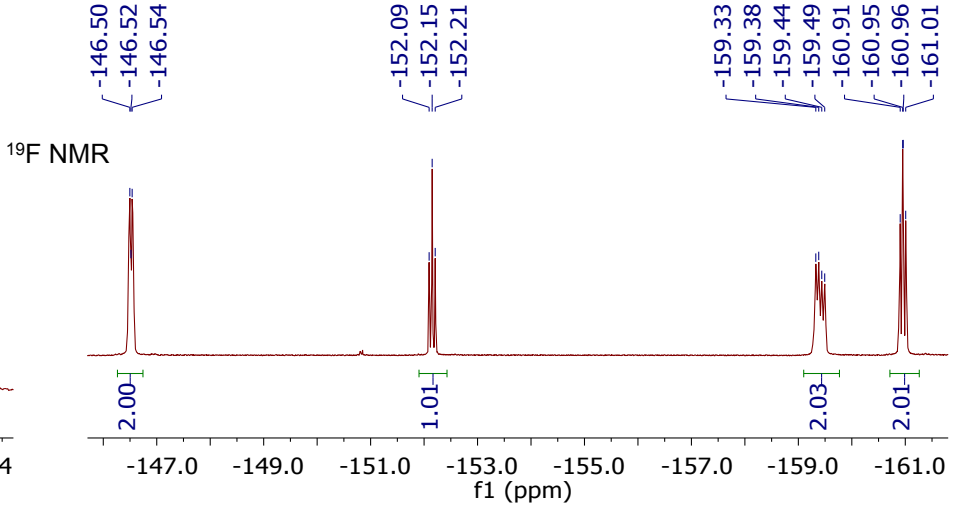

$[C_6F_5NNC(C_6F_5)NNMes]BF_2$ (1g)

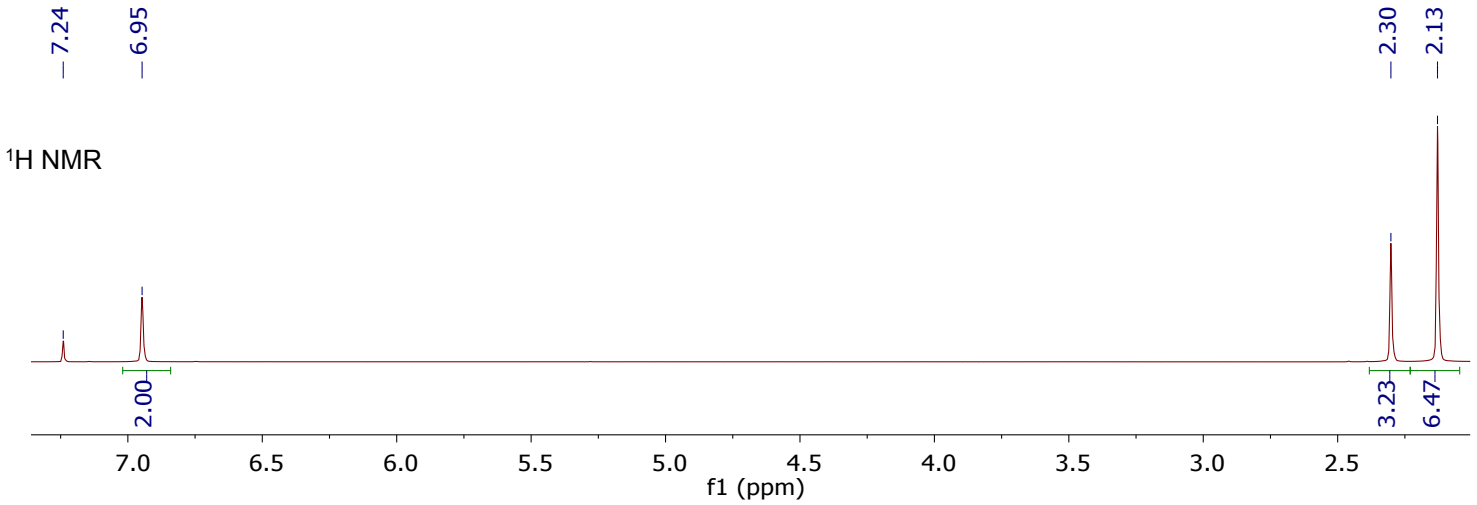

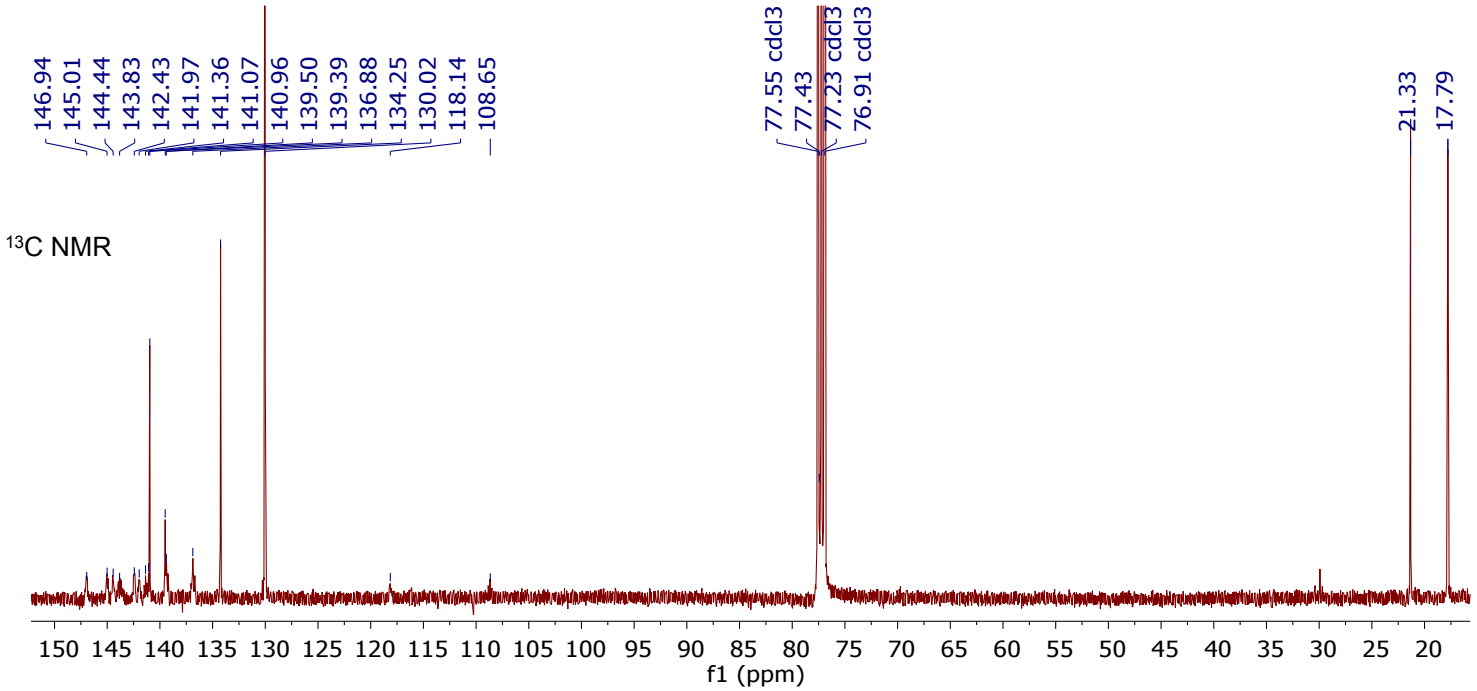

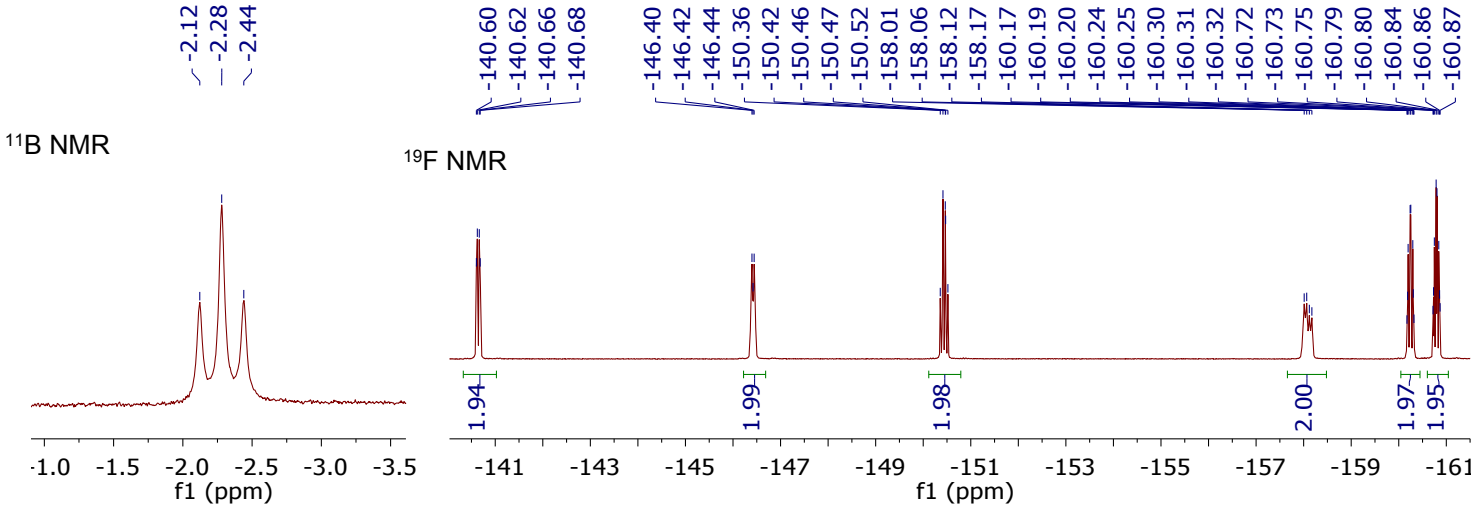

[PhNNC(CN(B(C_6F_5)$_3$))NNPh]BF_2 (1h^{BCF})

^{1}H NMR

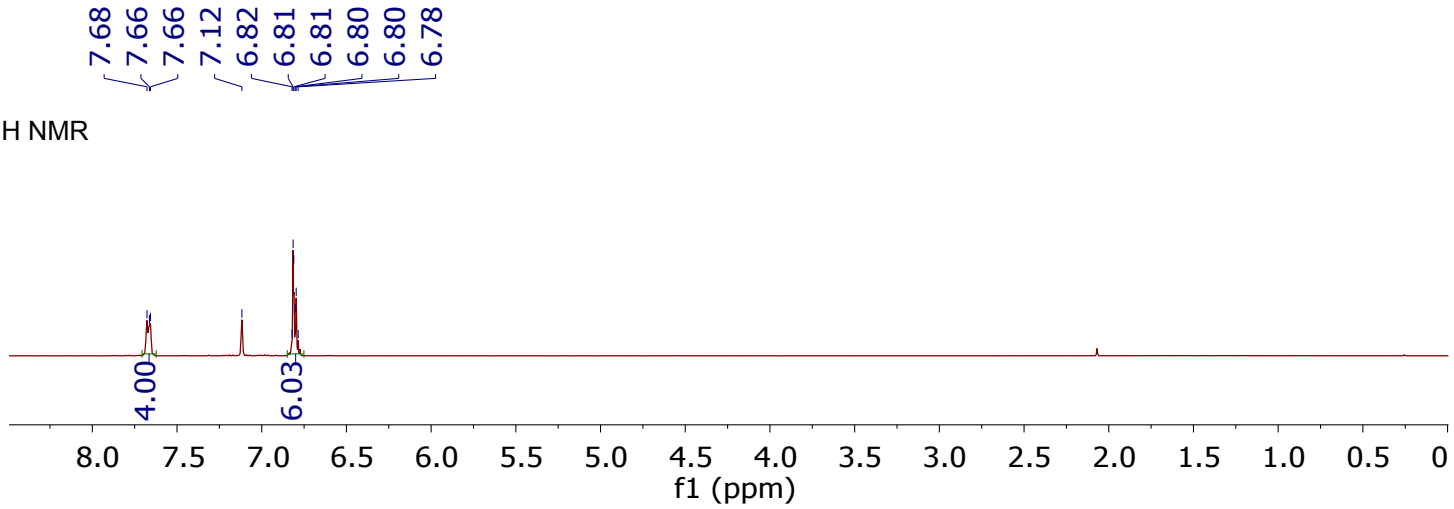

^{13}C NMR

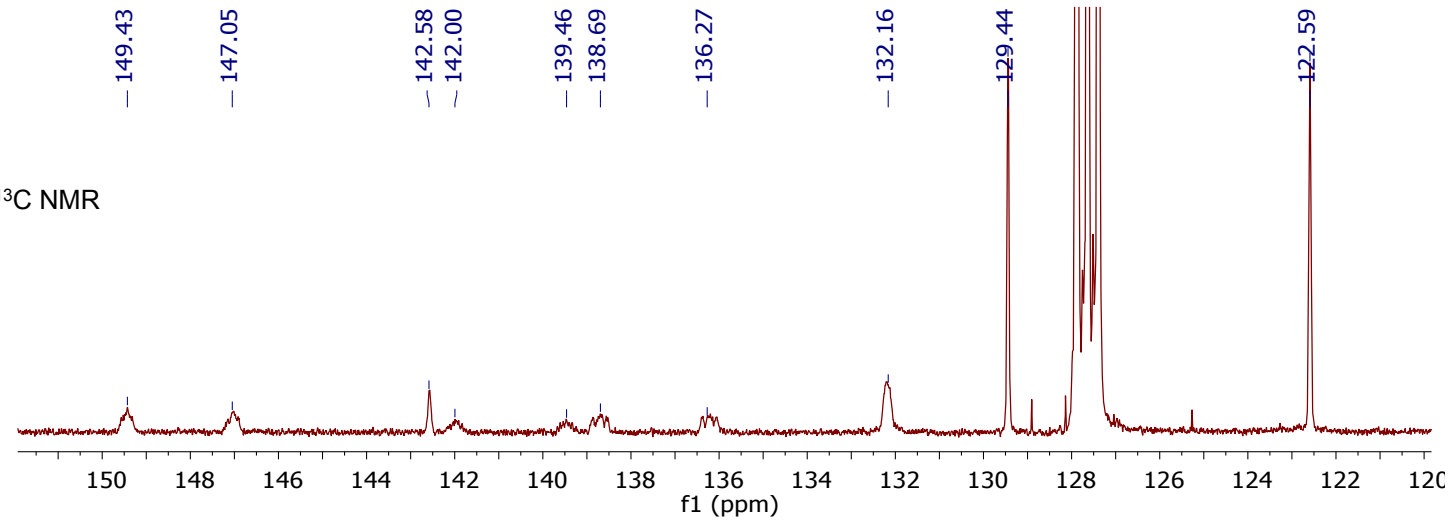

^{11}B NMR

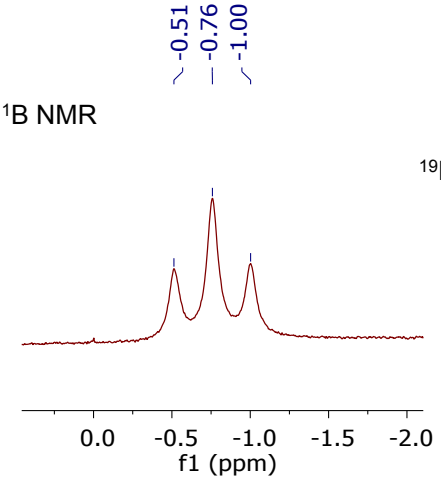

^{19}F NMR

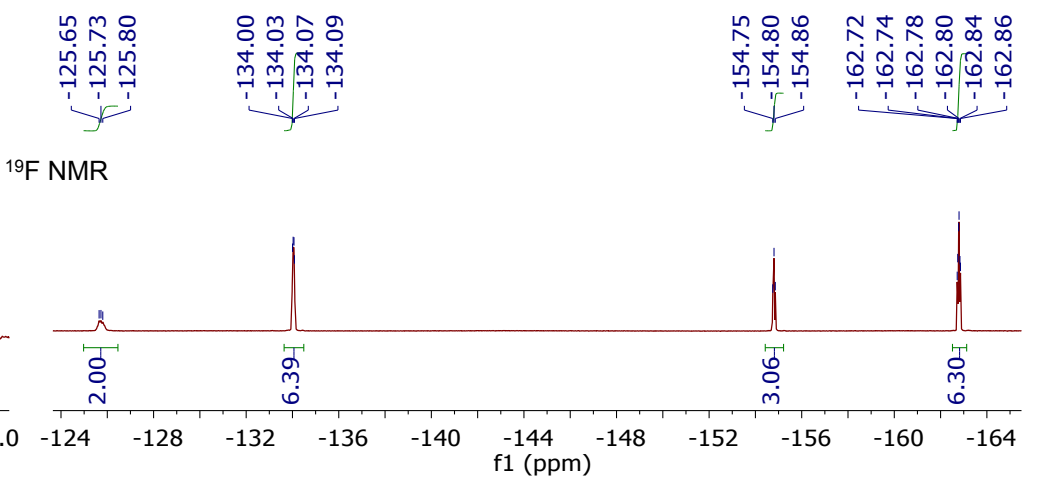

[MesNNC(CN)NNMes]BF_2 (1i)

^{1}H NMR

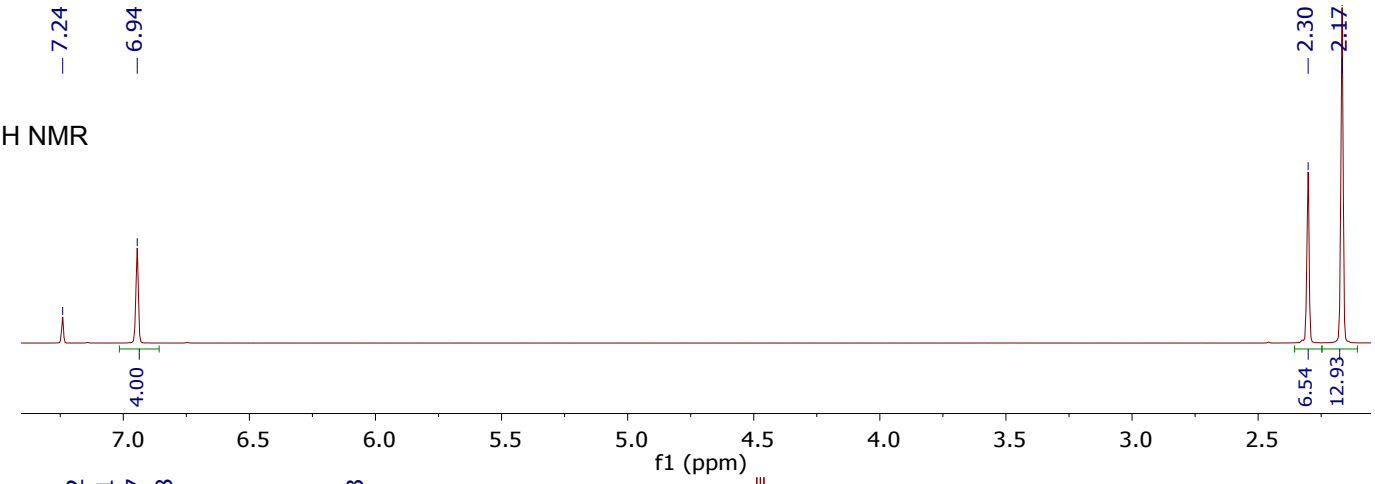

^{13}C NMR

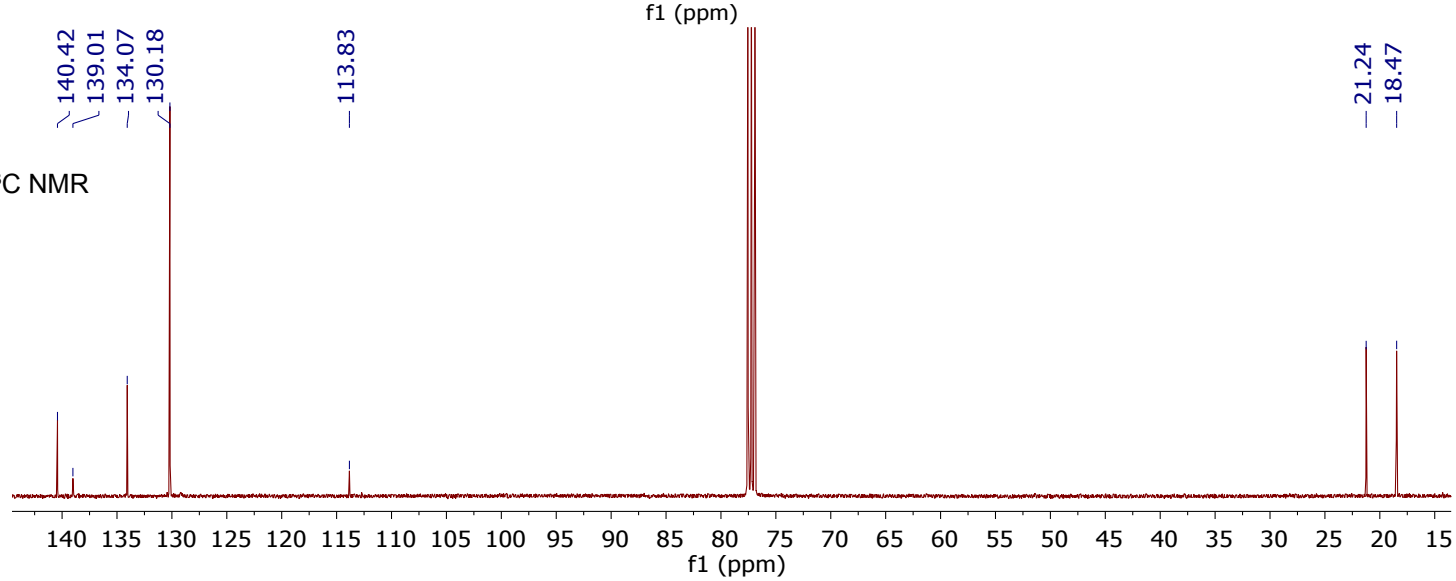

^{11}B NMR

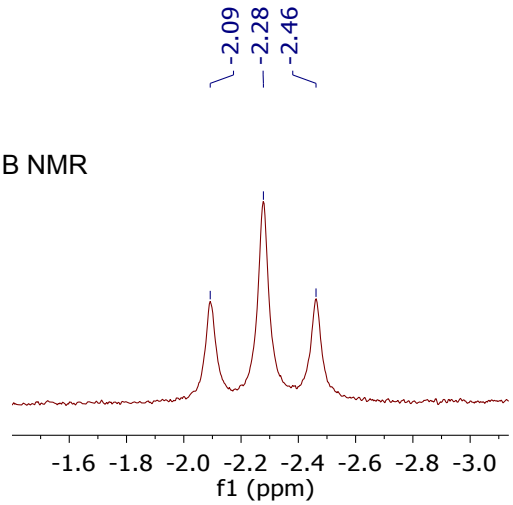

^{19}F NMR

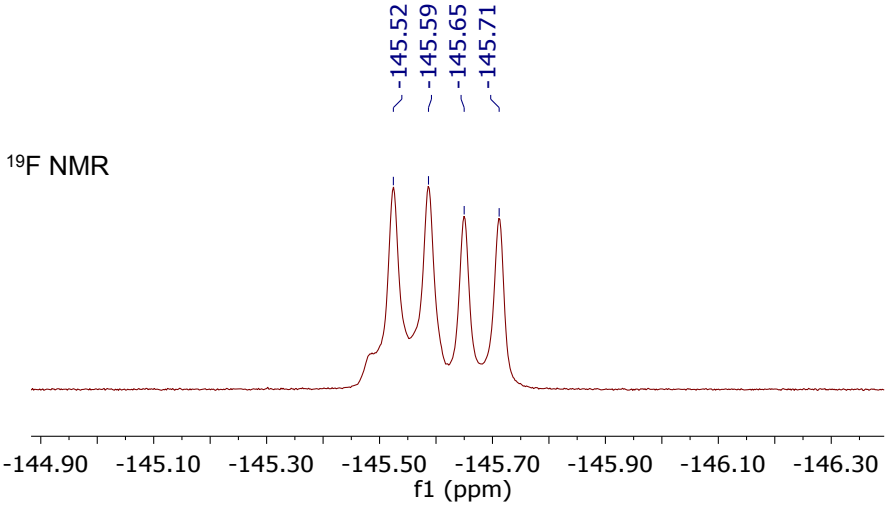

X-ray crystallography

Suitable crystals were mounted on a cryo-loop in a drybox and transferred, using inert-atmosphere handling techniques, into the cold nitrogen stream of a Bruker D8 Venture diffractometer. The final unit cell was obtained from the xyz centroids of 9403 (**1b**), 9967 (**1d**), 9954 (**1i**), 9895 (**1h^{BCF}**), 9745 ([Na(15-c-5)]$^+$**[1c]$^{\bullet-}$**), 9965 ([Cp_2Co]$^+$**[1f]$^{\bullet-}$**), and 9958 ([Cp^*_2Co]$^+_2$**[1j]$^{2\bullet-}$**) reflections after integration. Intensity data were corrected for Lorentz and polarisation effects, scale variation, for decay and absorption: a multiscan absorption correction was applied, based on the intensities of symmetry-related reflections measured at different angular settings (*SADABS)*.[24] The structures were solved by direct methods using the program *SHELXS*.[25] The hydrogen atoms were generated by geometrical considerations and constrained to idealised geometries and allowed to ride on their carrier atoms with an isotropic displacement parameter related to the equivalent displacement parameter of their carrier atoms. Structure refinement was performed with the program package *SHELXL*.[25] For **1h^{BCF}**, from the refinement it was clear that there were three regions of disordered residual density, one of which was identified as a toluene molecule. Some atoms in the toluene solvate molecule showed unrealistic displacement parameters when allowed to refine freely; DELU/SIMU restraints were applied. The other density in the other two regions could not be satisfactorily fit to solvent molecules, and ultimately the PLATON/SQUEEZE routine was used to remove this contribution. For [Cp^*_2Co]$^+_2$**[1j]$^{2\bullet-}$**, from the refinement it was clear that a toluene solvent molecule was disordered over an inversion centre. In addition, electron density was observed in a second void (probably disordered THF), which was masked using the PLATON/SQUEEZE routine. One of the Cp^*_2Co cations showed rotational disorder: a two-site model was applied with equivalent site occupancy factors. The anisotropic displacement parameters for the CH_3 groups in the two disorder components were constrained to be equivalent (EADP). For ([Na(15-c-5)]$^+$**[1c]$^{\bullet-}$**), from the solution it was clear that only one of the two independent molecules in the unit cell was well-defined. The other molecule suffered from severe disorder in the cationic part and the electron density in this part of the molecule appeared smeared out. A two-site occupancy model was applied for this fragment, with the S.O.F. for the major fraction refining to 0.51. Some atoms (including the Na atom in this fragment) showed unrealistic displacement parameters, which were constrained to have anisotropic displacement parameters equivalent to one of the neighboring atoms (EADP).

Crystal data and details on data collection and refinement are presented in Tables S1 and S2.

Table S1. Crystallographic data for compounds **1b**, **1d**, **1h^{BCF}** and **1i**.

	1b (CCDC 1471287)	**1d** (CCDC 1471288)	**1h^{BCF}** (CCDC 1471295)	**1i** (CCDC 1471293)
chem formula	$C_{17}H_{19}BF_2N_4$	$C_{20}H_{12}BF_7N_4$	2 $(C_{32}H_{10}B_2F_{17}N_5)(C_7H_8)$ [a]	$C_{20}H_{22}BF_2N_5$
M_r	328.17	452.15	1710.27 [a]	381.23
cryst syst	orthorhombic	monoclinic	monoclinic	orthorhombic
color, habit	orange, block	red, block	orange, block	Yellow, needle
size (mm)	0.30 x 0.10 x 0.08	0.35 x 0.31 x 0.04	0.32 x 0.23 x 0.07	0.33 x 0.04 x 0.03
space group	*Pnma*	*P21/c*	*C 2/c*	*Pnma*
a (Å)	16.6601(5)	18.5945(8)	32.728(4)	5.9716(2)
b (Å)	17.4301(5)	7.3570(3)	8.7616(11)	17.0399(6)
c (Å)	5.6620(2)	14.5283	29.466(4)	18.8991(6)
α (°)				
β (°)		108.9680(10)	112.024(3)	
γ (°)				
V (Å^3)	1644.17(9)	1879.55(14)	7833.0(18)	1923.09(11)
Z	4	4	4	4
ρ_{calc}, g.cm^{-3}	1.326	1.598	1.450	1.317
Radiation [Å]	Mo K_α 0.71073	Mo K_α 0.71073	Mo K_α 0.71073	Mo K_α 0.71073
μ(Mo K_α), mm^{-1}	0.096	0.145	0.143	0.094
μ(Cu K_α), mm^{-1}				
F(000)	688	912	3400	800
temp (K)	100(2)	100(2)	100(2)	100(2)
θ range (°)	3.38-27.14	2.81-27.13	2.98-27.27	3.22-27.15
data collected (h,k,l)	-21:21; -22:22; -7:7	-23:23; -9:9; -18:18	-42:42; -11:11; -37:37	-7:7; -21:21; -24:24
min, max transm	0.6954, 0.7455	0.6733, 0.7455	0.6486, 0.7455	0.7013, 0.7455
rflns collected	24656	32581	67066	29576
indpndt reflns	1877	4156	8760	2201
observed reflns $F_o \geq 2.0\ \sigma\ (F_o)$	1551	3175	5118	1796
R(F) (%) (reflns)	3.39 (1551)	3.94 (3175)	8.41 (5118)	3.70 (1796)
wR(F^2) (%) (reflns)	8.22 (1877)	10.45 (4156)	20.69 (8760)	9.19 (2201)
GooF	1.089	1.020	1.030	1.020

weighting a,b	0.0363, 0.5435	0.0507, 0.9616	0.0647, 47.4872	0.0395, 1.1881
params refined	120	290	539	139
min, max resid dens	-0.224, 0.298	-0.214, 0.308	-0.358, 0.467	-0.255, 0.317

[a] The chemical formula, molecular weight (M_r), density, F(000) and absorption coefficient are calculated without the contribution of the masked solvent molecules.

Table S2. Crystallographic data for compounds **[Na(15-C-5)][1c]**, **[Cp_2Co][1f]** and **[Cp^*_2Co]$_2$[1j]**

	[Na(15-C-5)][1c] (CCDC 1471289)	**[Cp_2Co][1f]** (CCDC 1471291)	**[Cp^*_2Co]$_2$[1j]** (CCDC 1471292)
chem formula	$C_{33}H_{43}BF_2N_4NaO_5$	$C_{32}H_{26}BCoF_7N_4$	$C_{72}H_{84}B_2Co_2F_4N_8$ (C_7H_8) [a]
M_r	647.51	669.31	1369.08 [a]
cryst syst	monoclinic	monoclinic	triclinic
color, habit	green, block	green, plate	green, block
size (mm)	0.16 x 0.16 x 0.10	0.16 x 0.11 x 0.01	0.17 x 0.12 x 0.05
space group	*P21*	*P21/c*	*P-1*
a (Å)	11.0275(9)	15.6779(3)	11.6834(7)
b (Å)	12.8604(9)	24.3649(5)	12.0343(7)
c (Å)	23.3615(18)	15.2499(3)	16.1553(10)
α (°)			90.699(2)
β (°)	93.306(2)	93.9593(9)	105.390(2)
γ (°)			117.4381(17)
V (Å^3)	3307.6(4)	5811.4(2)	1919.5(2)
Z	2	8	1
ρ_{calc}, g.cm^{-3}	1.300	1.530	1.184
Radiation [Å]	Mo K_α 0.71073	Cu K_α 1.54178	Mo K_α 0.71073
μ(Mo K_α), mm^{-1}	0.106		0.488
μ(Cu K_α), mm^{-1}		5.302	
F(000)	1372	2728	722
temp (K)	100(2)	100(2)	100(2)
θ range (°)	2.93-26.37	4.57-65.30	3.33-27.33
data collected (h,k,l)	-13:13; -13:16; -29:29	-18:18; -28:28; -17:17	-15:15; -15:15; -20:20
min, max transm	0.6742, 0.7455	0.5549, 0.7526	0.700, 0.746
rflns collected	62330	54491	51822
indpndt reflns	12845	9905	8568
observed reflns $F_o \geq 2.0\ \sigma\ (F_o)$	11185	8395	7022
R(F) (%) (refns)	4.04 (11185)	3.42 (8395)	4.17 (7022)
wR(F^2) (%) (reflns)	8.78 (12845)	7.99 (9905)	10.58 (8568)
GooF	1.027	1.025	1.020
weighting a,b	0.0367, 1.1969	0.0320, 3.9578	0.0421, 1.7212
params refined	932	817	539
restraints	1		175
min, max resid dens	-0.189, 0.213	-0.231, 0.340	-0.380, 0.454

[a] The chemical formula, molecular weight (M_r), density, F(000) and absorption coefficient are calculated without the contribution of the masked solvent molecules.

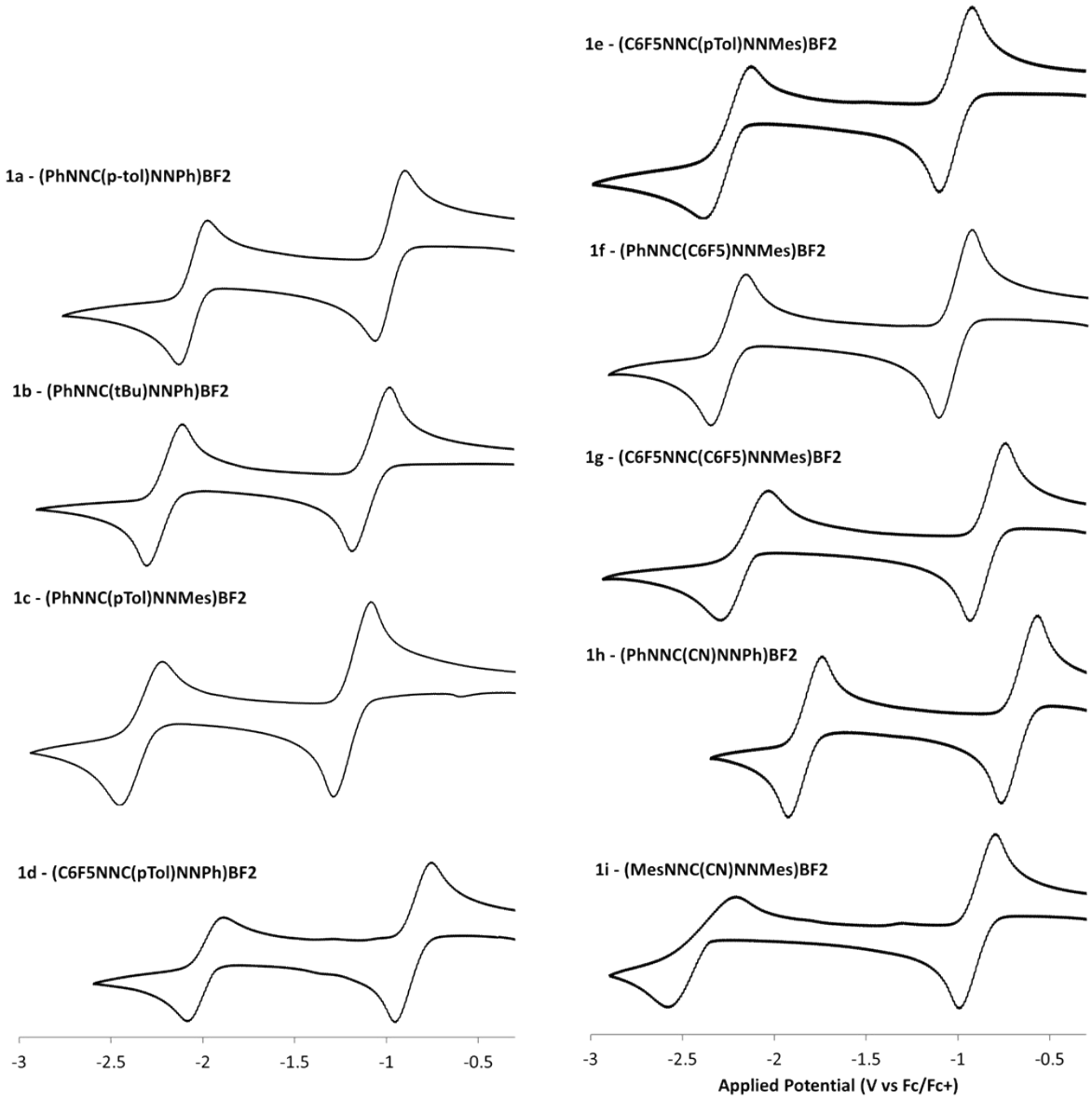

Figure S1. Cyclic voltammograms for compounds **1**.

Table S3. UV-Vis data of compounds $[1]^{\bullet-}$ in THF

	R_1	R_3	R_5	λ_{max} (nm)	ε (M^{-1} cm^{-1})
1a	Ph	p-Tol	Ph	454, 716	20893, 7372
1b	Ph	tBu	Ph	465, 668	15164, 6620
1c	Ph	p-Tol	Mes	448, 646	19283, 7178
1f	Ph	C_6F_5	Mes	399, 596	10580, 4056
1i	Mes	CN	Mes	378, 517	14657, 1069

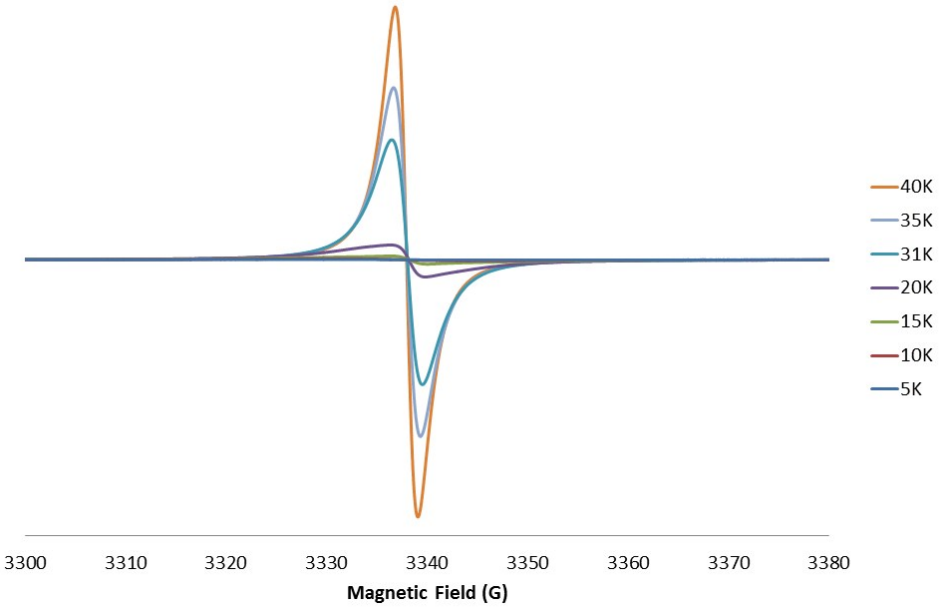

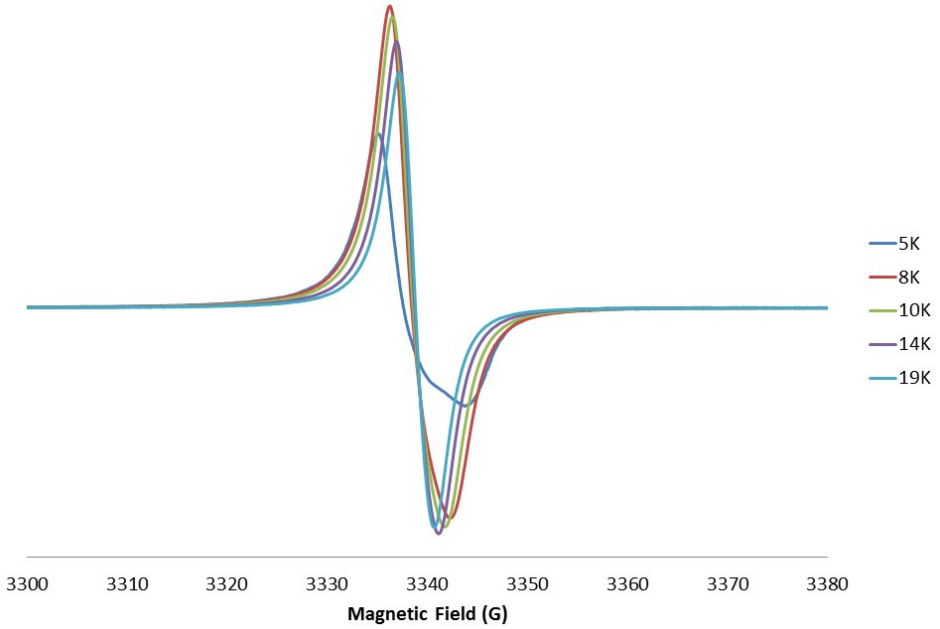

Figure S2. VT-EPR spectra of **$[Cp_2Co]^+_2[1j]^{2-}$** (top) and **$[Cp_2Co]^+_2[1k]^{2-}$** (bottom) in MeTHF/DMSO glass.

Computational details

Calculations to determine the electronic ground state of compound $[1j]^{2-}$ and $[1k]^{2-}$

Geometry optimizations for the reduced phenylene-linked compounds **$[1j]^{2-}$** and **$[1k]^{2-}$** were carried out at the B3LYP/6-31g(d) level. Closed-shell singlet, open-shell singlet and triplet states were calculated and their energies compared (Table S4). In line with the VT-EPR studies (see main text of the manuscript), **$[1j]^{2-}$** is calculated to have an open-shell singlet ('broken-symmetry') ground state, whereas **$[1k]^{2-}$** is calculated to have a triplet ground state.

Table S4. Comparison of calculated electronic energies for **$[1j]^{2-}$** and **$[1k]^{2-}$**.

	$[1j]^{2-}$		**$[1k]^{2-}$**	
	HF energy (a.u.)	relative energies (kcal/mol)	HF energy (a.u.)	relative energies (kcal/mol)
closed-shell singlet	-2121.2498385	19.44	-2121.2436561	19.54
open-shell singlet	-2121.2811427	0	-2121.2745897	0.13
triplet	-2121.2808157	0.21	-2121.2747907	0

Computational results (geometries, transition energies) for 1 and $1^{\bullet-}$

The computational protocol follows the one described previously for reproducing band shapes and optical signatures of fluoroborates[7] and is it therefore only briefly summarized here. All DFT and TD-DFT were performed using the latest version of the Gaussian 09 program package,[8] applying a tightened self-consistent field convergence criterion (10^{-9}-10^{-10} a.u.) and an improved optimization threshold (10^{-5} au on average residual forces). In all DFT and TD-DFT calculations, the so-called *ultrafine* pruned (99,590) grid, was applied. The SOS-CIS(D) calculations have been determined with the Q-Chem package,[9] using the resolution of identity (RI) scheme.

First the geometrical and vibrational parameters of the ground-state were determined with DFT and the 6-31G(d) atomic basis set [LanL2DZ for the Co atom]. This basis set has been shown to provide accurate results for BODIPY-like compounds.[7b,10] For a few systems, the first excited-state geometry was determined with TD-DFT and the same basis set combination. Of course, all structures presented in the main text correspond to true minima of the potential energy surface (no imaginary frequencies). In a subsequent step, the transition energies between the two states have been determined at the TD-DFT and SOS-CIS(D) levels, both relying on the 6-311+G(2d,p) [LanL08(f) for the Co atom] atomic basis set (and a with a triple-ζ auxiliary basis set for the RI part).[10] All of DFT and TD-DFT calculations were carried out with the M06-2X exchange-correlation functional.[11] In order to take into account the conditions of experimental measurements, the DFT and TD-DFT calculations (geometry optimization, vibrational calculations and transition energies) were carried out in the presence of the solvent (here: THF), using the Polarizable Continuum Model (PCM)[12] in its corrected linear response (cLR) derivation for the excited-state energies.[13] In the main text, all transition energies (both absorption and emission) are obtained at the cLR-PCM-TD-DFT level and corrected by the difference between TD-DFT and SOS-CIS(D) gas-phase results. We redirect the readers to previous works for more details.[7] Calculations performed on the radical anion form of **1a** were made with the same computational protocol.

For **1a**, we have performed additional calculations in which the geometry was optimized with 6-31+G(d) whereas the transition energies were computed with 6-311++G(2df,2p). The difference in the absorption wavelengths was found to be ca. 4 nm, that is negligible at this level of theory. For the $[Cp_2Co]^{+}[1a]^{\bullet-}$ complex, we have also compared the UV/Vis spectra determined with an all-electron basis set and with the pseudopotential basis set and obtained completely similar simulated spectra.

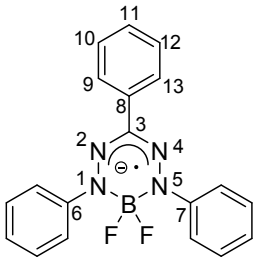

F

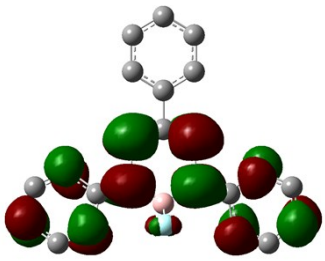

SOMO

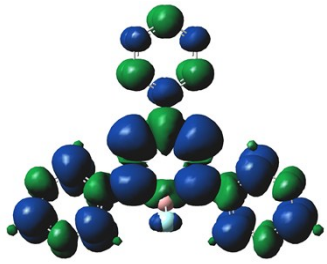

spin density

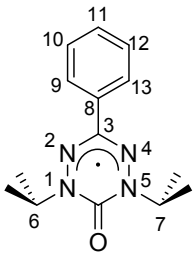

G

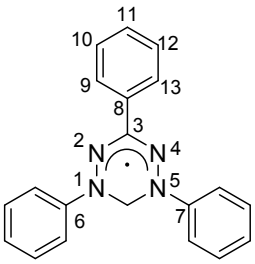

H

Table S5. Mulliken atomic spin densities for F, G, and H from DFT calculations at the B3LYP/6-31G(d) level of theory

	F	G	H		F	G	H
N1	0.179	0.191	0.167	C8	0.028	0.036	0.032
N2	0.322	0.412	0.364	C9	-0.027	-0.032	-0.029
C3	-0.145	-0.169	-0.159	C10	0.018	0.020	0.018
N4	0.331	0.414	0.372	C11	-0.028	-0.030	-0.028
N5	0.182	0.191	0.170	C12	0.018	0.020	0.018
C6	-0.040	-0.012	-0.043	C13	-0.027	-0.032	-0.029
C7	-0.041	-0.012	-0.045				

Table S5. Calculated isotropic hyperfine coupling constant (hfcc) in Gauss for F, G and H from DFT calculations at the B3LYP/EPR-III level of theory

	F	G	H
N1	2.79	3.98	3.78
N2	4.59	5.82	5.09
N4	4.59	5.82	5.09
N5	2.79	3.98	3.79
B	-3.69		
F	-0.80		
F	-1.44		

References

(1) Chang, M.-C.; Roewen, P.; Travieso-Puente, R.; Lutz, M.; Otten, E. *Inorg. Chem.* **2015**, *54*, 379.
(2) Chang, M. C.; Otten, E. *Chem. Commun.* **2014**, *50*, 7431.
(3) Barbon, S. M.; Reinkeluers, P. A.; Price, J. T.; Staroverov, V. N.; Gilroy, J. B. *Chem. Eur. J.* **2014**, *20*, 11340.
(4) (a) Gilroy, J. B.; Ferguson, M. J.; McDonald, R.; Patrick, B. O.; Hicks, R. G. *Chem. Commun.* **2007**, 126. (b) Gilroy, J. B.; Otieno, P. O.; Ferguson, M. J.; McDonald, R.; Hicks, R. G. *Inorg. Chem.* **2008**, *47*, 1279.
(5) Barbon, S. M.; Price, J. T.; Yogarajah, U.; Gilroy, J. B. *RSC Advances* **2015**, *5*, 56316.
(6) Barbon, S. M.; Price, J. T.; Reinkeluers, P. A.; Gilroy, J. B. *Inorg. Chem.* **2014**, *53*, 10585.
(7) (a) Chibani, S.; Laurent, A. D.; Le Guennic, B.; Jacquemin, D. *J. Chem. Theory Comput.* **2014**, *10*, 4574. (b) Le Guennic, B.; Jacquemin, D. *Acc. Chem. Res.* **2015**, *48*, 530.
(8) Frisch, M. J.; Trucks, G. W.; Schlegel, H. B.; Scuseria, G. E.; Robb, M. A.; Cheeseman, J. R.; Scalmani, G.; Barone, V.; Mennucci, B.; Petersson, G. A.; Nakatsuji, H.; Caricato, M.; Li, X.; Hratchian, H. P.; Izmaylov, A. F.; Bloino, J.; Zheng, G.; Sonnenberg, J. L.; Hada, M.; Ehara, M.; Toyota, K.; Fukuda, R.; Hasegawa, J.; Ishida, M.; Nakajima, T.; Honda, Y.; Kitao, O.; Nakai, H.; Vreven, T.; Montgomery Jr., J. A.; Peralta, J. E.; Ogliaro, F.; Bearpark, M. J.; Heyd, J.; Brothers, E. N.; Kudin, K. N.; Staroverov, V. N.; Kobayashi, R.; Normand, J.; Raghavachari, K.; Rendell, A. P.; Burant, J. C.; Iyengar, S. S.; Tomasi, J.; Cossi, M.; Rega, N.; Millam, N. J.; Klene, M.; Knox, J. E.; Cross, J. B.; Bakken, V.; Adamo, C.; Jaramillo, J.; Gomperts, R.; Stratmann, R. E.; Yazyev, O.; Austin, A. J.; Cammi, R.; Pomelli, C.; Ochterski, J. W.; Martin, R. L.; Morokuma, K.; Zakrzewski, V. G.; Voth, G. A.; Salvador, P.; Dannenberg, J. J.; Dapprich, S.; Daniels, A. D.; Farkas, Ö.; Foresman, J. B.; Ortiz, J. V.; Cioslowski, J.; Fox, D. J., *Gaussian 09, Revision D.01*, **2009**, Gaussian, Inc.
(9) Shao, Y.; Gan, Z.; Epifanovsky, E.; Gilbert, A. T. B.; Wormit, M.; Kussmann, J.; Lange, A. W.; Behn, A.; Deng, J.; Feng, X.; Ghosh, D.; Goldey, M.; Horn, P. R.; Jacobson, L. D.; Kaliman, I.; Khaliullin, R. Z.; Kuś, T.; Landau, A.; Liu, J.; Proynov, E. I.; Rhee, Y. M.; Richard, R. M.; Rohrdanz, M. A.; Steele, R. P.; Sundstrom, E. J.; Woodcock, H. L.; Zimmerman, P. M.; Zuev, D.; Albrecht, B.; Alguire, E.; Austin, B.; Beran, G. J. O.; Bernard, Y. A.; Berquist, E.; Brandhorst, K.; Bravaya, K. B.; Brown, S. T.; Casanova, D.; Chang, C.-M.; Chen, Y.; Chien, S. H.; Closser, K. D.; Crittenden, D. L.; Diedenhofen, M.; DiStasio, R. A.; Do, H.; Dutoi, A. D.; Edgar, R. G.; Fatehi, S.; Fusti-Molnar, L.; Ghysels, A.; Golubeva-Zadorozhnaya, A.; Gomes, J.; Hanson-Heine, M. W. D.; Harbach, P. H. P.; Hauser, A. W.; Hohenstein, E. G.; Holden, Z. C.; Jagau, T.-C.; Ji, H.; Kaduk, B.; Khistyaev, K.; Kim, J.; Kim, J.; King, R. A.; Klunzinger, P.; Kosenkov, D.; Kowalczyk, T.; Krauter, C. M.; Lao, K. U.; Laurent, A. D.; Lawler, K. V.; Levchenko, S. V.; Lin, C. Y.; Liu, F.; Livshits, E.; Lochan, R. C.; Luenser, A.; Manohar, P.; Manzer, S. F.; Mao, S.-P.; Mardirossian, N.; Marenich, A. V.; Maurer, S. A.; Mayhall, N. J.; Neuscamman, E.; Oana, C. M.; Olivares-Amaya, R.; O'Neill, D. P.; Parkhill, J. A.; Perrine, T. M.; Peverati, R.; Prociuk, A.; Rehn, D. R.; Rosta, E.; Russ, N. J.; Sharada, S. M.; Sharma, S.; Small, D. W.; Sodt, A. *Mol. Phys.* **2015**, *113*, 184.
(10) Chibani, S.; Le Guennic, B.; Charaf-Eddin, A.; Maury, O.; Andraud, C.; Jacquemin, D. *J. Chem. Theory Comput.* **2012**, *8*, 3303.
(11) Zhao, Y.; Truhlar, D. G. *Theor. Chem. Acc.* **2007**, *120*, 215.
(12) Tomasi, J.; Mennucci, B.; Cammi, R. *Chem. Rev.* **2005**, *105*, 2999.
(13) Caricato, M.; Mennucci, B.; Tomasi, J.; Ingrosso, F.; Cammi, R.; Corni, S.; Scalmani, G. *J. Chem. Phys.* **2006**, *124*, 124520.